Activity report at the Lake Monoun for the depressions on the bottom

[1]Takeshi OHBA, [1]Seigo Ooki, [1]Yu Oginuma, [2]Issa, [2]Alain Fouepe, [2]Mbassogog Zachee
[1]Tokai University, Japan
[2]IRGM, Cameroon

Aim of the activity

The survey by the multibeam sonar at Lake Monoun in Nov 2014 revealed the detailed feature of the bottom shape of lake. Lake Monoun is composed of the three basins, West, Central and East. TheEeast basin is the largest and deepest basin. On the bottom of East basin, two depressions were found. The depressions were expected to be the outlets of fluid containing magmatic components. The aim of activity at Lake Monoun is to disclose the identity of depressions.

Observation at the depressions

On 28th Feb and 1st Mar 2015, the observation for the depressions were carried out using a rubber boat with the aide of handheld GPS pointer and a rope. First of all, point a2 (Fig 1) was searched with the aide of GPS. The end of a light blue vinyl rope, which floats on water, was tied to a dead wood on water surface (Fig 2a). Another end of rope was tied to the central working raft. Moving along the rope, with the aid of GPS, the point a1 was located. At the point a1, CTD casting and water sampling by use of Niskin sampler and MK sampler were carried out. As same as the point a1, the point b1 was located by use of rope and GPS. One end of the rope was tied to a dead wood on water surface (Fig 2b). Another end of rope was tied to the raft of pumping system with a solar panel.
For the comparison with the water in depressions, one or two neighboring points were located and CTD castings were carried out. For the standard of lake water, a CTD casting was also given at the central working raft. The real point of observation has the coordinate slightly shifted from the a1 and b1 due to the movement of boat by wind. Therefore, the point of observation on depressions is defined to be D1 and D4 instead of a1 and b1, respectively. The points D1, D4 with the neighboring points and the central point C are shown in Fig 3.

Results

The temperature profiles of the observation points are drawn in Fig 4a and 4b. The electric conductivity profiles are drawn in Fig 5a and 5b. The pH profiles are drawn in Fig 6a and 6b. As show in Fig 4a, 5a and 6a the profiles of each points substantially overlap in the range shallower than -96m. In the range deeper than -96m at D1, significantly high temperature and conductivity were observed (Fig.4b and Fig. 5b) relative to the neighboring points (D2 and D3) or C. At D4, a slightly high temperature was observed relative to the neighboring point D5. The depth at D4 reached nearly -102m. At D1, the electric conductivity deeper than -96m was significantly higher than the standard lake water at C (Fig 5b). At D4, a similar increase was found which started at -99m. The increase turned to decrease at -101m. The profile of pH in deep region is interesting (Fig 6b). The normal lake water shows an increasing trend along the increase of depth. However, pH at D1 decreased at -97m suddenly. At D4, an excess increase was found in the range deeper than -99m.

The main component of carbonaceous species in lake water in the deeper region is CO_{2aq}. The electric conductivity proportional to $[HCO_3^-]$, the concentration of HCO_3^-. For the estimation of $[CO_{2aq}]$, the following equilibrium is assumed.

$$CO_{2aq} + H_2O = H^+ + HCO_3^- \qquad (1)$$

The equilibrium of eq-1 gives us,

$$[CO_{2aq}] = 10^{-pH}[HCO_3^-]K_1^{-1} \qquad (2).$$

Where K_1 is the equilibrium constant of eq-1, which depends on temperature. The following correlation is assumed between $[HCO_3^-]$ and electric conductivity, C_{25}.

$$[HCO_3^-] = k\, C_{25} \qquad (3)$$

Where k is a proportional constant. Combining eq-2 and 3, the following expressions are given.

$$[CO_{2aq}] = k\, C_{25}\, 10^{-pH} K_1^{-1} \qquad (4)$$

$$[CO_{2aq}] + [HCO_3^-] = k\, C_{25}\, (10^{-pH} K_1^{-1} + 1) \qquad (5)$$

In Fig 7, the evaluated right hand side (RHS) of eq-4 and 5 excluding k value are plotted along the depth at D1 and D4. A clear enrichment of CO_{2aq} and HCO_3^- are indicated at D1 in the range deeper than -97m. A slight enrichment was also confirmed at D4. In the enriched fluid at D1, $[CO_{2aq}]$ occupies about 80% within the summation of $[CO_{2aq}]$ and $[HCO_3^-]$.

Conclusions

In the region deeper than -97m at D1, a hot fluid significantly enriched in CO_{2aq} and HCO_3^- was detected. In the region deeper than -99m at D4, a fluid similar to that at D1 was detected although the enrichment relative to the normal lake water is not high. The lake water sampled in the enriched region at D1 will be analyzed in Japan. The existence of enriched hot fluid in the depression at D1 and D4 suggests that the depressions are the outlet of fluid containing magmatic component.

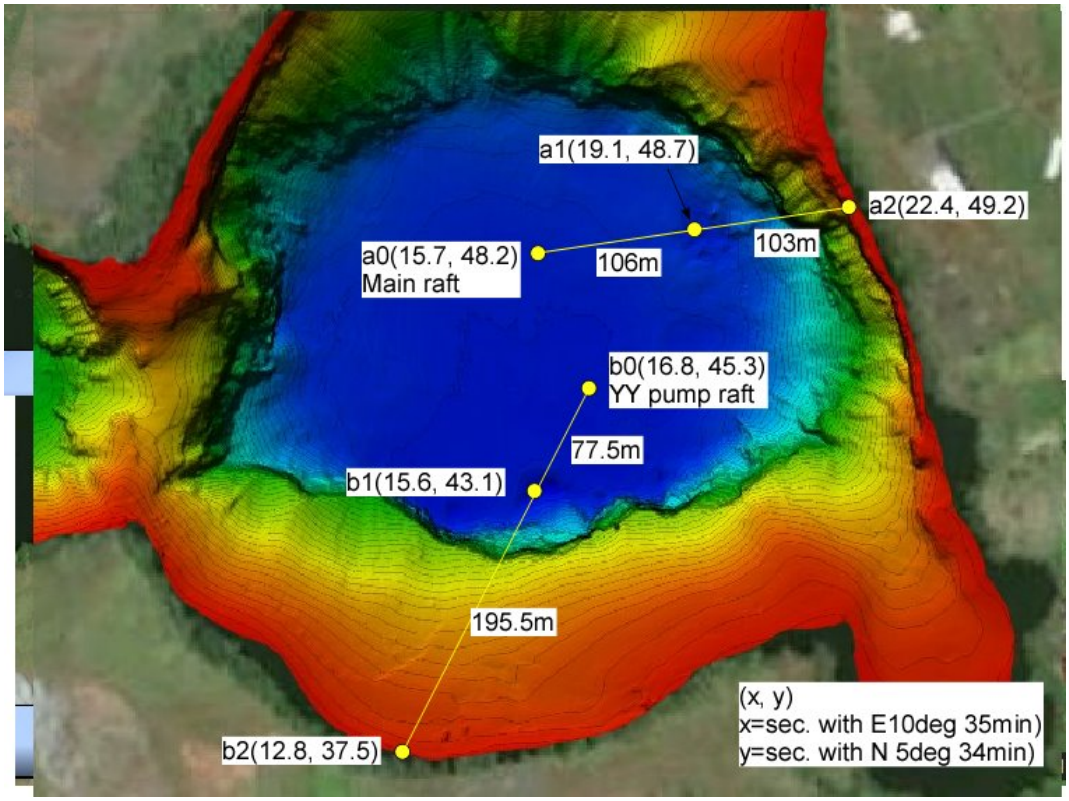

Fig.1. Map of Lake Monoun to locate the two depressions. The values in parenthesis indicate the second after degree and minute in longitude and latitude.

Fig.2a Point a2 where the end of rope was tied to a dead wood.

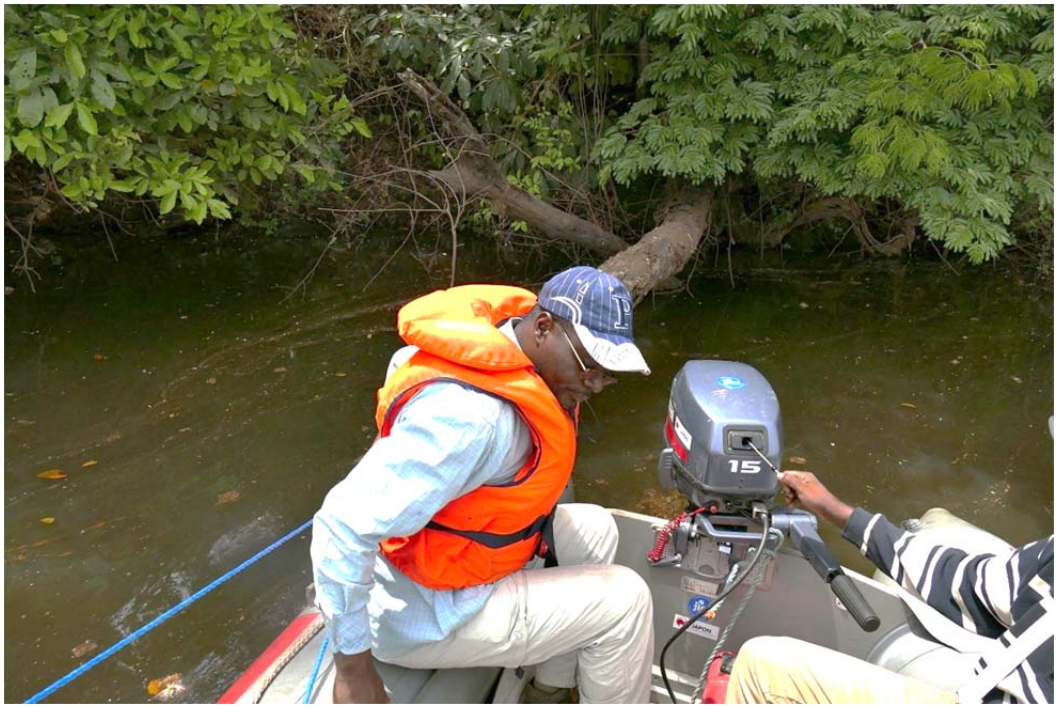

Fig.2b. Point b2 where the end of rope was tied to a dead wood.

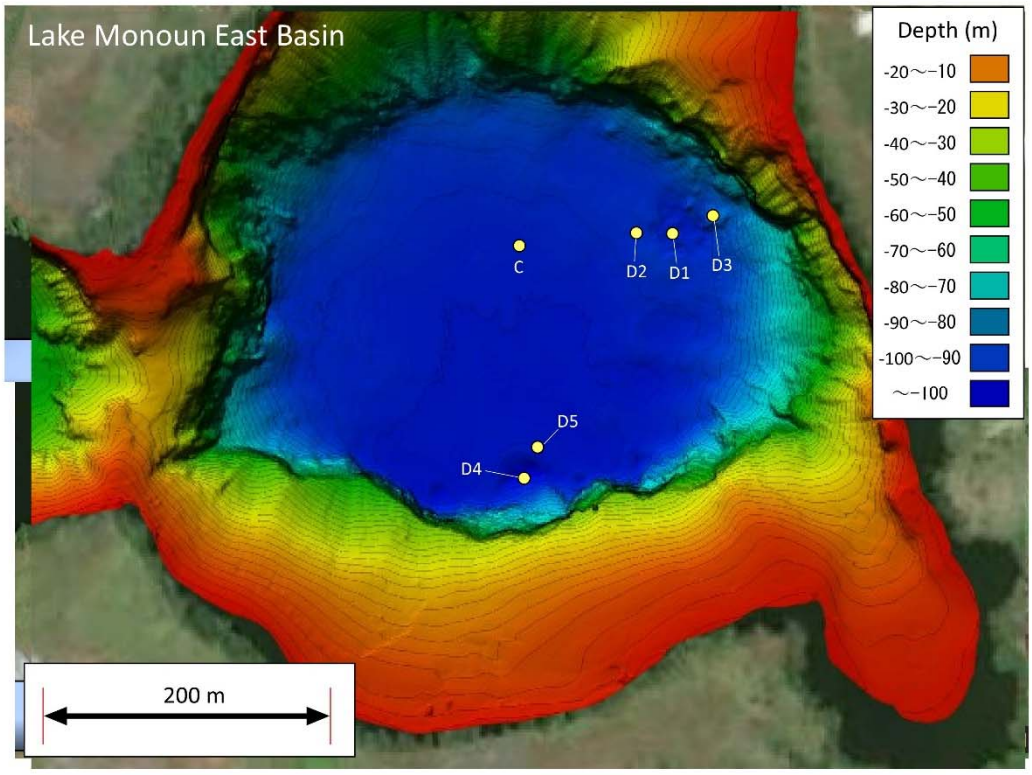

Fig.3. Real location of the CTD castings

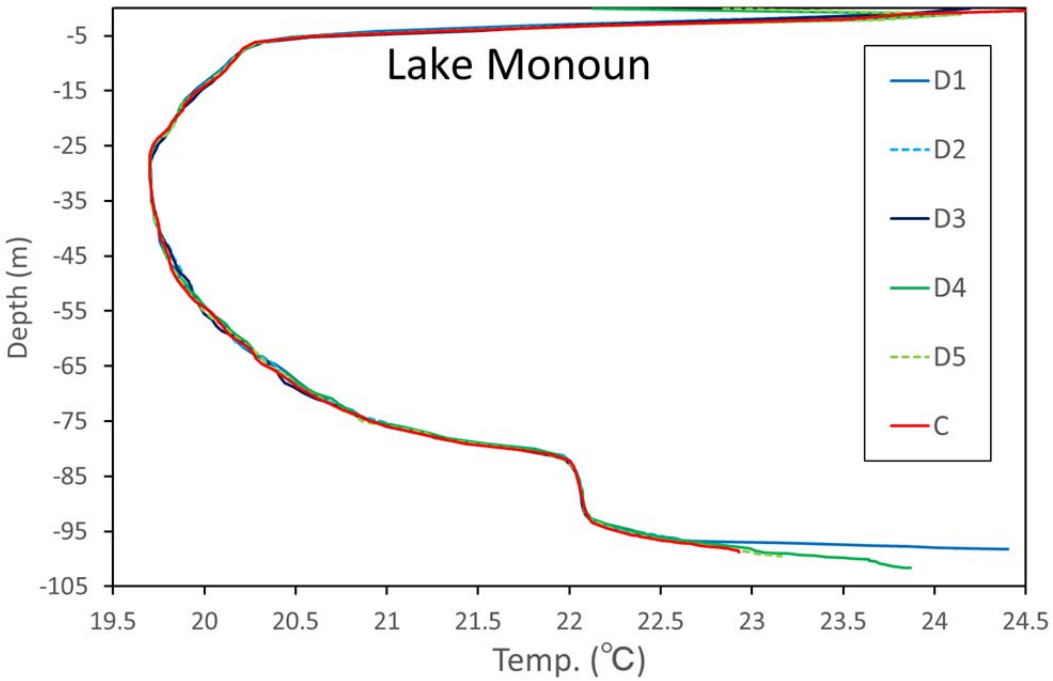

Fig.4a. Temperature profile at the observation points

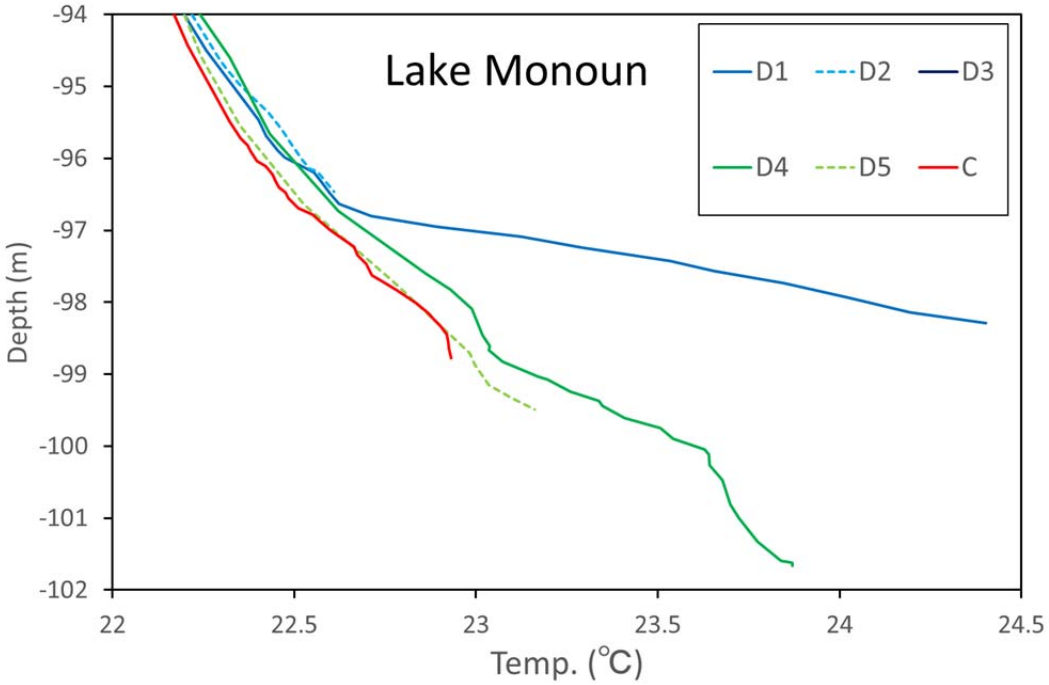

Fig.4b. Temperature profiles for the enlargement in deep part

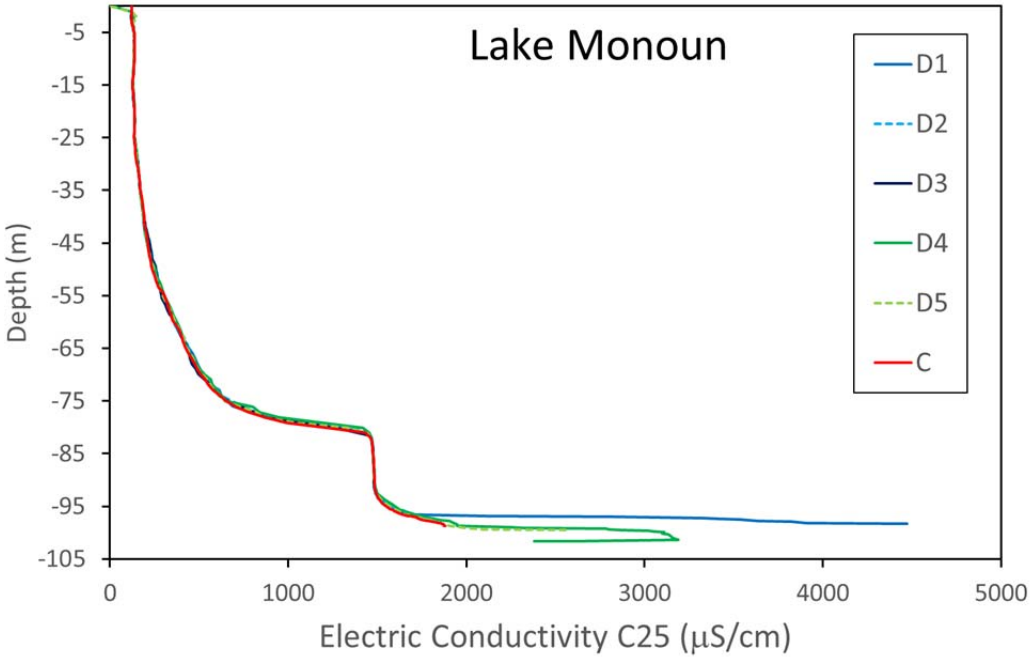

Fig.5a. Electric conductivity profile at the observation points.

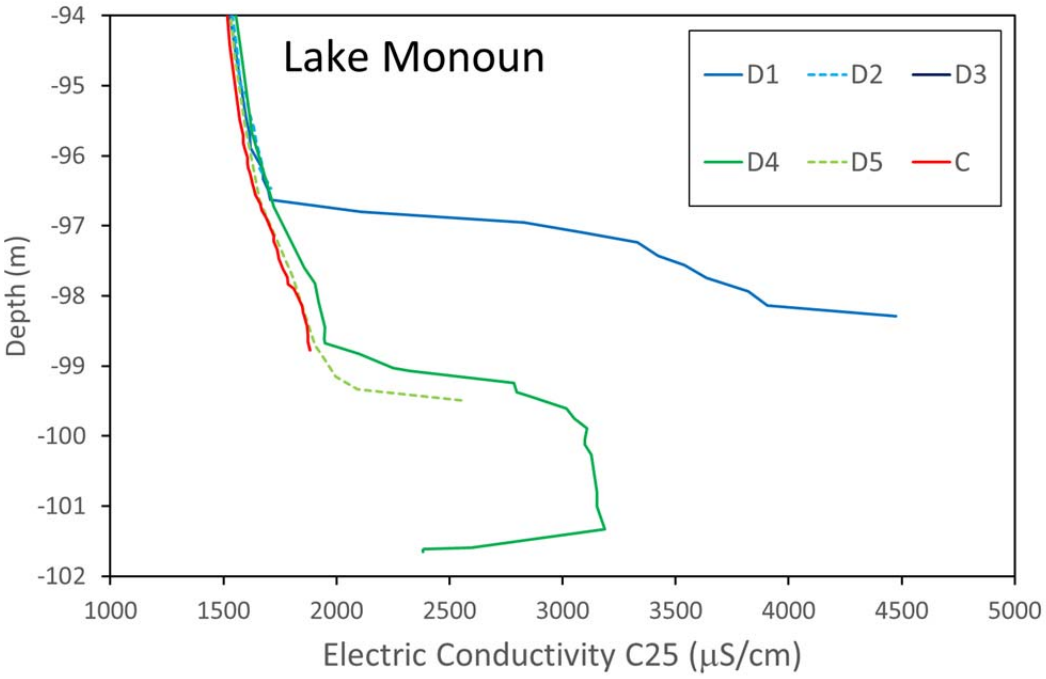

Fig.5b. Electric conductivity profile for the enlargement in deep part

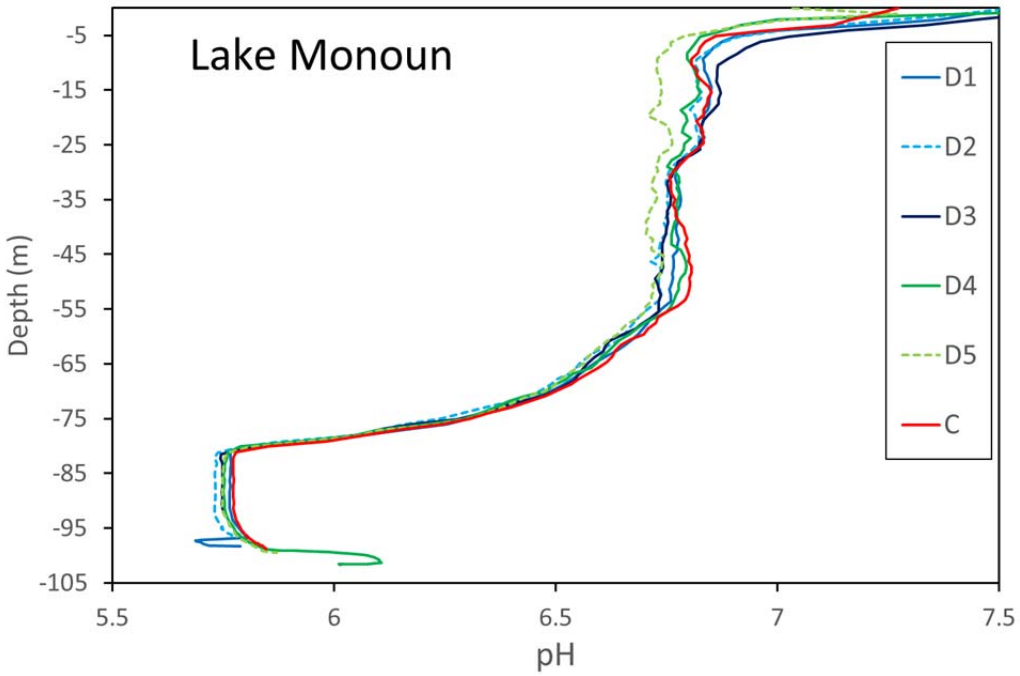

Fig.6a. pH profiles at the observation points

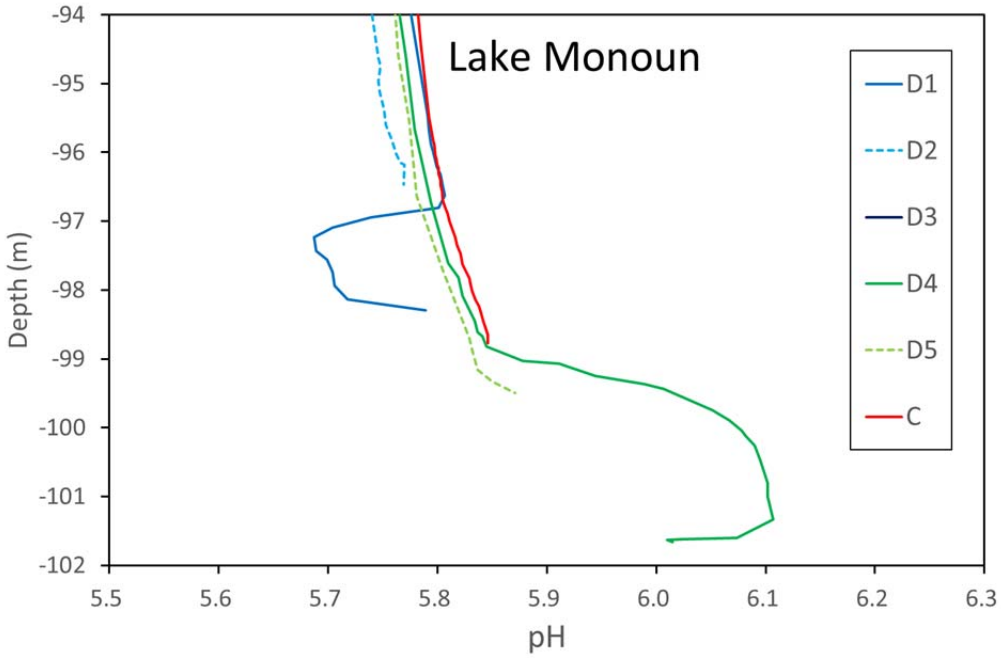

Fig.6b. pH profiles for the enlargement in deep part

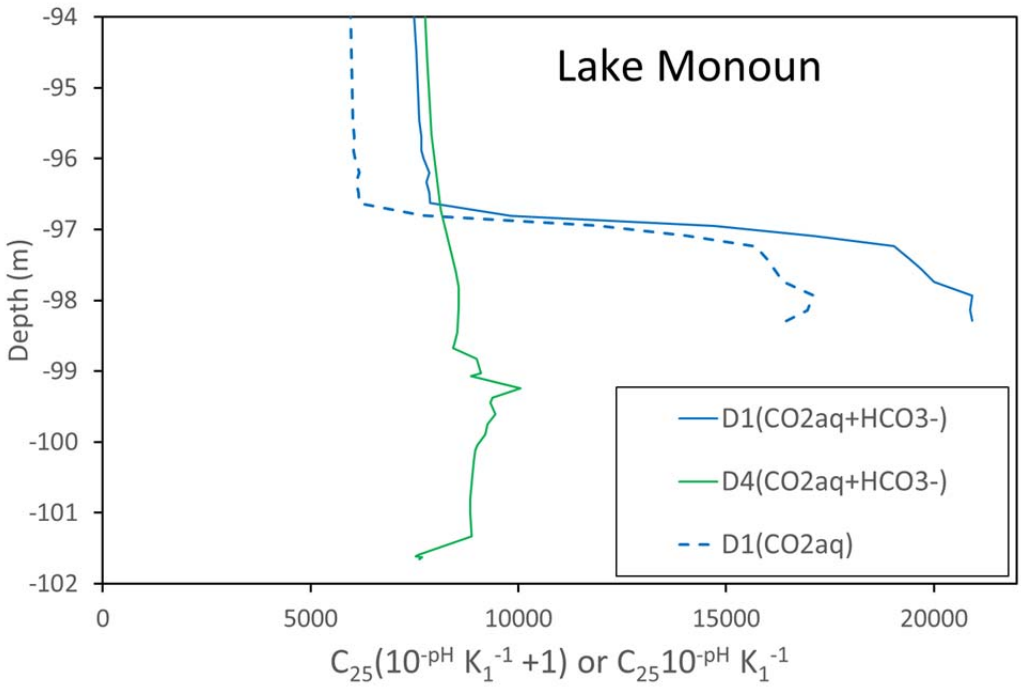

Fig.7. Profile of RHS in eq-4 and 5 excluding k value, which is proportional to the concentration of CO_{2aq} and $CO_{2aq}+HCO_3^-$, respectively.